



IEA Bioenergy
Technology Collaboration Programme

Gasification applications in existing infrastructures for production of sustainable value-added products

Case Study 3: Integration of renewables into existing refineries

IEA Bioenergy: Task 33

December 2021





IEA Bioenergy

Technology Collaboration Programme

Gasification applications in existing infrastructures for production of sustainable value-added products

Case study 3: Integration of renewables into existing refineries

Authors: Reinhard Rauch, Xhesika Korovesi

Karlsruher Institut für Technologie

Acknowledgement: Frank Schäfer, Jens Wilms

IEA Bioenergy: Task 33

December 2021

Copyright © 2021 IEA Bioenergy. All rights Reserved

Picture at front of the document courtesy from MiRO Mineraloelraffinerie Oberrhein (2021) and Shutterstock/FotoIdee.

Published by IEA Bioenergy

Abstract

This report discusses the possibilities for integration of gasification systems into conventional oil refineries for the production of synthetic bio-fuels. The long-term integration concept of these bio-fuels in existing refineries generally usually envisions the synthesis of a raw intermediate product off-site or decentral and it's further processing and upgrading to end synthetic fuels central or on-site. However, in this report the complete synthesis pathway of the bio-fuels is studied on-site in the refinery by using one of Germany's largest refineries, Mineraloelraffinerie Oberrhein (MiRO), as an example.

The discussed synthetic fuels belong to the second generation of bio-fuels which utilize feedstocks such as woody biomass, agriculture waste and other non-food lignocellulosic biomass for the gasification process. The production pathway of bio-fuels in a biorefinery begins with the conversion of biomass through the pyrolysis and gasification processes into a synthesis gas, which serves as feed for the further synthesis of bio-fuels. The purification and conditioning steps of the synthesis gas based on the requirements of the subsequent synthesis unit follow.

In this study the implementation of the Fischer-Tropsch process and the Methanol/DME-to-Gasoline processes was considered. These processes differ in yield and quality of produced bio-fuel, so that the Fischer-Tropsch is more adequate for the synthesis of high-quality diesel components, whereas the Methanol/DME-to-Gasoline processes for the production of high-quality gasoline components. In addition, the processing and upgrading of the synthetic fuel components into the refinery structures differs according the applied process. The product derived from the Fischer-Tropsch process is separated in the atmospheric distillation unit and upgraded to intermediate and final products through the refinery structures. The processing of the wax fraction in this study was considered in two ways: conversion into lighter boiling fractions through fluid catalytic cracking or through a hydrocracker in the presence of H_2 . The products derived from the Methanol/DME-to-Gasoline processes on the other hand need to be conditioned and processed only in a stabilization column of the refinery to produce a high-quality gasoline blend comparable in quality with reformat.

The yield target of 50 t/h of product feed to the refinery system (syncrude or raw gasoline blend) was set and used in the evaluation of the mass and energy balances in this study. The efficiency of the processes was analysed through the energy efficiency factors (η , $\eta_{products}$, η_{total}), where the energy of the synthetic fuel, by-products and overall steam and fuel gas production are compared to the energy of the biomass feedstock, respectively. The Fischer-Tropsch process with the implementation of a hydrocracker unit was shown to produce higher yields of diesel components compared to the catalytic cracking and also a higher overall energy efficiency. It could also be concluded that the Methanol/DME-to-Gasoline processes deliver lower synthetic fuel energy efficiencies compared to the Fischer-Tropsch process. Amongst the Methanol-to-Gasoline and DME-to-Gasoline processes, the DtG process could deliver a higher yield of synthetic gasoline, so also a higher synthetic fuel energy efficiency compared to the MtG process, but the product and overall energy efficiency of the MtG process were shown to be higher.

Lastly an economic analysis of the different integration pathways into the refinery was performed. The integration of the Fischer-Tropsch process resulted to be slightly more economic than the Methanol/DME-to-Gasoline processes. In addition, it could be concluded that the Biomass-to-Liquid route analysed in this report is much more economic than the Power-to-Liquid route for synthetic fuel production in Germany. The latter could however be competitive in the case of electricity production in the MENA regions.

List of contents

The conventional oil refinery and the possible integration of renewables.....	4
Mineraloelraffinerie oberrhein (Miro), as a conventional oil refinery	4
Integration pathways for synthetic fuels into the refinery structures	6
Feedstock for the production of synthetic fuels	7
Gasification system and biofuel synthesis unit	8
Fischer-Tropsch process	9
Methanol-to-Gasoline and DME-to-Gasoline processes.....	10
Material and Energy balances	13
Fischer-Tropsch process	14
Methanol-to-gasoline and DME-to-gasoline processes.....	16
Economic analysis of the integration into the refinery	18
Appendices.....	21
Appendix 1 - Tables.....	21
Appendix 2 - Figures & Further details.....	27
Index of Tables	30
Index of Figures	31
Publication bibliography.....	32

The conventional oil refinery and the possible integration of renewables

In the recent decades the importance of renewable energy sources has become crucial in regard to the global climate crisis resulting from high greenhouse gas emissions. To reverse the consequences of this climate crisis, an energy transformation process has been undertaken in many countries, such as the European Green Deal of the European Union. The energy transformation process aims the creation of an extensive greenhouse gas neutral economy and society, which focuses on the principles of a sustainable utilization of resources and the conservation of biodiversity, by the year 2050 (BMW 2010). This concept includes all the sectors of the energy system, important part of which is the transportation sector with an emission contribution of around 20 % (Dietrich et al. 2018). For the sustainability of the transportation sector, it is widely accepted that the sectors of air and freight transportation will have to operate on liquid synthetic fuels, due to the high energetic density that they provide (Dietrich et al. 2018). Therefore, the utilization of synthetic fuels remains essential for a sustainable future and needs to be further researched so that it can be employed on the long term.

Conventional crude oil refineries need to integrate synthetic fuels into their structures in order to effectively reduce their greenhouse gas emissions in the long term and become independent from the limited energy raw material, i.e., crude oil. According to the expert discussions, the coupling of advanced synthetic fuels into the conventional refinery processes is already possible today up to one fifth, with minor adjustments in the plant configuration. In Germany, for example this would imply the substitution of around 20 million tonnes of currently processed crude oil with synthetic crude, i.e., syn crude. (Hobohm et al. 2018)

MINERALOELRAFFINERIE OBERRHEIN (MIRO), AS A CONVENTIONAL OIL REFINERY

One of the main refineries in Germany is Mineraloelraffinerie Oberrhein GmbH & Co. KG, abbreviated as MiRO, which processes about 15 million tonnes of crude oil annually, 15 % of the total amount of processed crude oil in Germany (MWV 2017). MiRO produces a wide range of products, from transportation and industrial fuels to chemical feedstock. The transportation fuels, diesel and gasoline, represent the biggest share of the production. Other products of MiRO include bitumen and calcinate, used in the road construction and aluminium production, respectively, but also hydrocarbons such as butane, propylene, benzene etc. used as feedstock for the chemical industry. A flowsheet of the refinery structures and processes of MiRO is displayed in Figure 1 and will be followingly described in detail.

The production path within the oil refinery starts with the crude oil, which after a desalting process is fed to the atmospheric distillation unit, where the thermal separation of the light and heavy components occurs. In the overhead of the atmospheric distillation column, light gases along with LPG are obtained, which are further processed to respectively be used as refinery gas for the internal energy demands at MiRO and as end products: butane, propane, propylene etc. The gasoline-boiling range obtained from the distillation process, also known as the straight-run gasoline, is the simplest gasoline component to be produced, but the yield naturally supplied from the crude oil does not meet the high qualitative and quantitative demands for conventional gasoline (Alfke et al. 2003), which is why it needs to be further catalytically upgraded. The gasoil fraction obtained from the atmospheric distillation unit on the other hand does not require any additional upgrading processes.

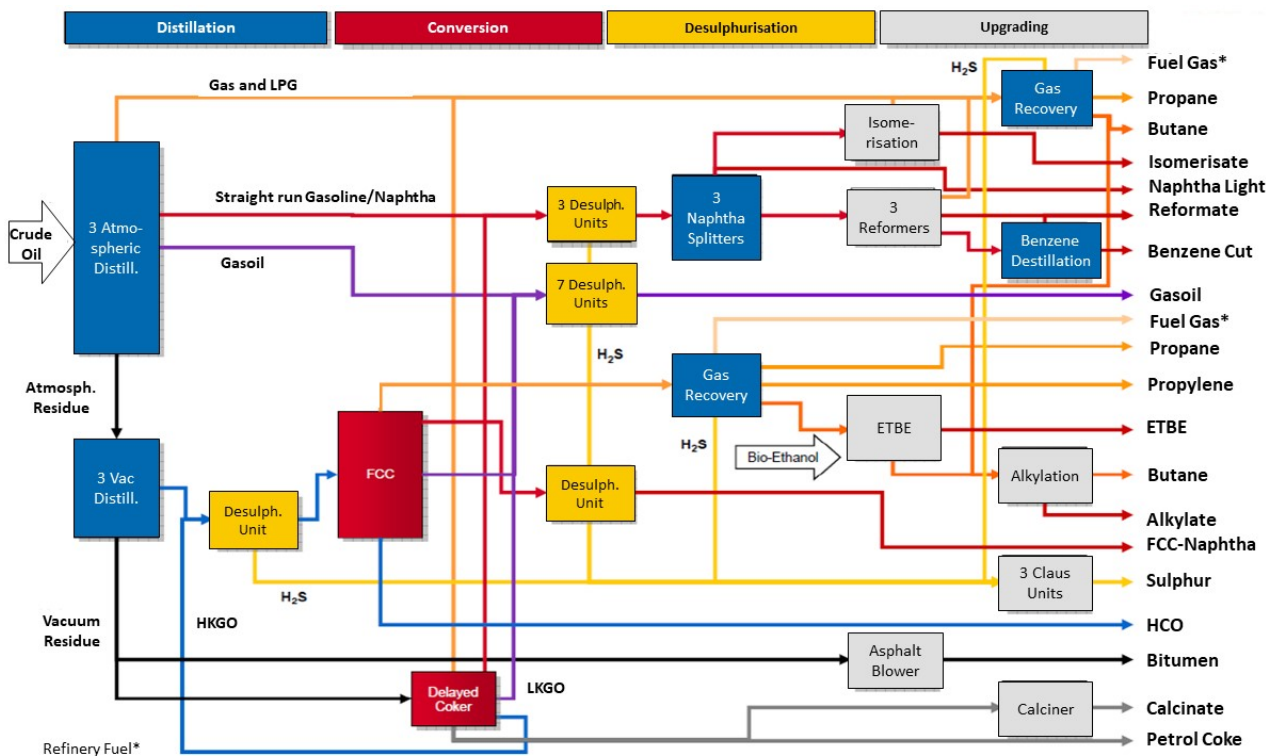


Figure 1. Block diagram of main refinery structures at MiRO.

Nevertheless, a desulphurisation of both the gasoline and gasoil fractions is necessary due to the sulphur content restriction in the combustion fuels specifications (DIN EN 228:2017-08; DIN EN 590:2017-10). In addition, the desulphurisation step is required prior to all upgrading processes in the refinery, in order to avoid a catalyst poisoning later in the reactors. The atmospheric residue obtained at the bottom of the atmospheric distillation unit is followingly fed into the vacuum distillation column and is separated at under-atmospheric pressures into the lighter vacuum gasoil and heavy vacuum residue. The vacuum gasoil is catalytically cracked in a fluidized catalytic cracker (FCC) in order to obtain high amounts of the gasoline-boiling range fractions and gasoil, along with light gases and heavy gasoil (HCG). The majority of the heavy vacuum residue from the crude oil on the other hand, is thermally cracked in the delayed coker resulting in the production of heavy coker gasoil (HKGO), light coker gasoil (LKGO), petroleum coke and light gases. The remaining part of the heavy vacuum residue is used in the production of bitumen.

The processing of the gasoil fraction at MiRO includes only the previously discussed desulphurisation step, mandatory due to the commercial diesel blend specifications. The processing of the gasoline fraction however, requires additional upgrading process to reach the required quality specifications of the commercial gasoline blend. This is the reason why today in a refinery, there are many gasoline components, such as catalytically cracked gasoline (FCC-Naphtha), catalytic reformat, isomerate and alkylate, each with different characteristics and a different blending proportion in the conventional gasoline. The gasoline upgrading structures at MiRO: the isomerisation unit, the catalytic reformers and the alkylation unit are presented in the block diagram of Figure 1.

In the catalytic reformer, the gasoline fractions obtained from the naphtha splitters after the atmospheric distillation unit are converted into a high-octane reformat with high content of aromatics under the production of hydrogen. This produced hydrogen is a very valuable component in other refinery processes such as e.g., desulphurization. Reformat contains also

an elevated amount of benzene, which is restricted in conventional gasoline and that is why it is separated and further delivered to the chemical industry. Because of its high-octane quality (RON \approx 96-99) this gasoline component has a major role in the production of high-octane gasoline. The isomerization unit produces a lower octane quality component (RON \approx 88) compared to reformate, known as isomerate, with mainly C₅-C₆ isoparaffins, which is nevertheless very desirable and an important gasoline blending-stock. Another attractive gasoline component consisting of isoparaffins is alkylate, which has moderately high octane quality (RON \approx 90 - 94) and is produced from the combination of light olefins, coming from the fluidized catalytic cracker (FCC) with isobutane (Gary et al. 2020). Alkylate is used along with isomerate to achieve and compensate for the gasoline octane quality that cannot be reached with reformate due to its aromatic nature (Alfke et al. 2003).

INTEGRATION PATHWAYS FOR SYNTHETIC FUELS INTO THE REFINERY STRUCTURES

The production and integration of synthetic fuels into the processing structures of the refinery is a crucial step in the reduction of greenhouse gas emissions so that a sustainable future of the mobility can be achieved. The long-term integration concept of these renewably derived fuels in existing refineries generally envisions the synthesis of the raw intermediate product off-site and the processing and upgrading to the synthetic fuel on-site. In this study the calculations are based on the assumption of a complete synthesis process on-site in the refinery. Depending on the desired type, yield and quality of the produced synthetic fuel the Fischer-Tropsch process or the Methanol/DME-to-Gasoline processes can be implemented.

- The **Fischer-Tropsch (FT)** process is a direct catalytic synthesis pathway and results in a so-called syncrude, consisting of a wide linear hydrocarbon product distribution, which is highly dependent on the reaction conditions. However, the process chemistry of the low temperature FT process is best suited for the synthesis of **high-quality diesel** rather than for the synthesis of gasoline-boiling range hydrocarbons of a high quality (Gogate 2018; Jung et al. 2020). For this reason, the FT process has the key-role as a synthetic diesel production pathway for integration in a bio-refinery.
- The **Methanol/DME-to-Gasoline (MtG/DtG)** processes are indirect catalytic synthesis pathways with MeOH/DME as intermediates and deliver a product spectrum of paraffins, olefins and mainly methyl-substituted aromatics with a maximum carbon number of C₁₀, which make it a **high-quality gasoline** blend (Chang and Silvestri 1977; Liederman et al. 1982). This is why the MtG and DtG processes are mainly considered for integration into a refinery, when the production focuses on a high-quality synthetic gasoline blend.

The FT raw product can be treated in the refinery as a synthetic crude oil and be fed similarly to the conventional crude oil into the atmospheric distillation unit, to be followingly processed in the respective refinery structures. The main end product is expected to be diesel with gasoline and light hydrocarbons as by-products.

The MtG and DtG processes produce a raw product, which is comparable in quality and composition to the reformate of the catalytic reformer in the refinery. This can enable an integration of the MtG/DtG raw product directly into the reformate upgrading structures at the refinery and offers a synthetic option for the conventional reformate, which constitutes an important gasoline blending component.

Feedstock for the production of synthetic fuels

The first generation of bio-fuels, such as ethanol and bio-diesel from oil containing crops, are heavily debated, because their primary feedstock derives from food crops and therefore is in direct competition to the food production industry. The second generation of bio-fuels i.e., the synthetic fuels discussed in this report, are fuels that utilize feedstocks such as woody biomass, agriculture waste, sewage sludge, municipal waste and other non-food lignocellulosic biomass. Lignocellulose is the abundant construction material of the cell walls of all terrestrial plants and contributes almost 90% to the available land biomass, which is why its use in the form of residues and wastes from agriculture, forestry etc. is a versatile feedstock for the second generation bio-fuel production through the gasification process (Dahmen et al. 2017). The simplified average composition of lignocellulose is about 40-55 wt.-% cellulose fibers, 15-35 wt.-% hemicellulose and 20-40 wt.-% lignin, represented by $C_6H_8O_4$ as approximate sum formula.

The characteristics and physical properties of these synthetic fuels are similar to conventional gasoline and diesel, but with the benefit of lower emissions from the engines of vehicles (Dabelstein et al. 2003). Additionally, their application in regular internal combustion engines is possible without further modifications (Haro et al. 2013). A similarity of the synthetic fuels to conventional fossil fuels is advantageous, because it would enable a gradual deployment of these synthetic fuels with minimum supply disruption (Tunå and Hulteberg 2014).

The production of synthetic fuels begins with the generation of a highly reactive gas mixture composed of H_2 and CO , which is known as synthesis gas i.e., syngas. In the concept of a biorefinery this can occur through the Biomass-to-Liquid (BtL) route, where a variety of residual biomass and other organic residues can be converted through the pyrolysis and gasification processes to result in a synthesis gas. Alternatively, the Power-to-Liquid (PtL) route is applicable for the production of syngas through the utilization of renewable electricity for water electrolysis and of captured CO_2 as feedstock. The conditioned synthesis gas from both routes can followingly be used in the Fischer Tropsch, Methanol-to-Gasoline or DME-to-Gasoline processes, depending on the required yields and synthetic fuel type. Both of the above-mentioned routes and their combination (PBtL) are presented in Figure 2 along with the downstream processes.

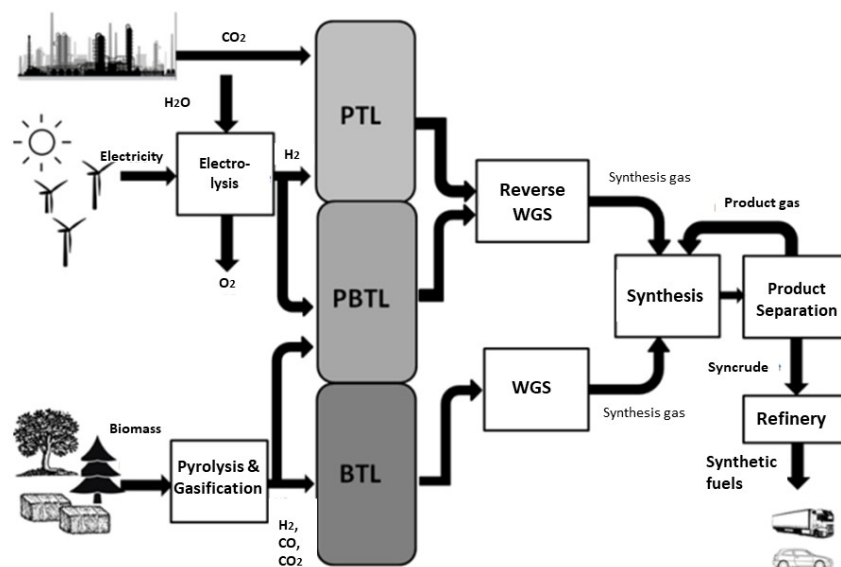


Figure 2. Summary of different pathways for the production of synthetic fuels.

A crucial benefit that the BtL route offers in comparison to the PtL route is the wide variety of

applicable feedstock (straw, hay, residual wood, sewage residues etc.), which depending on the region could be a very advantageous property. In addition, despite the wide range of results found in different literature sources a gasification system seems to offer to date a more economically convenient route for integration into a biorefinery compared to the PtL route, for e.g., in the study of Hannula (2015).

In this report the focus lies on the BtL route, which is why the following calculations and results consider only a gasification system for the syngas production. Whereas, the PtL route will not be discussed in detail in this report and is mentioned only for comparison purposes and in order to offer a complete summary of the synthetic fuel production pathways.

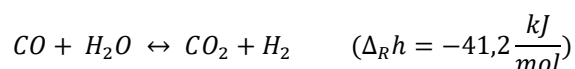
Gasification system and biofuel synthesis unit

As gasification system, the bioliq® process is used in this study. The lignocellulosic biomass feedstock is firstly dried at the entrance of the gasification system and then decomposed in a fast pyrolysis plant into an energy-dense intermediate (suitable for economic transport over long distances) at the temperature of around 500 °C. The products of the pyrolysis are mainly liquid, whereas the produced light gases are usually burned to achieve the reaction temperature of the reactor. (Dahmen et al. 2017)

The mixture of pyrolysis oil and pyrolysis coke is preheated and pumped into a pressurized entrained flow gasifier, where in the presence of pure oxygen and water steam it is converted at 1200°C into a raw synthesis gas containing mainly H₂, CO, CO₂ and H₂O. Oxygen-blown gasification is preferred to air-blown gasification, since in the latter nitrogen can act as an inert diluent and result in a decreasing overall process efficiency. So even though oxygen gasification is associated with higher capital costs, this is usually justified due to the higher synthetic fuel yields due to higher syngas quality (Dimitriou et al. 2018).

There is a variety of gasification reactor types, but in this study the entrained flow gasifier was chosen because it offers advantages such as the control of hydrocarbon formation, the highest capacity per unit volume and the raw gas product is almost free of tar and phenols. These are due to the higher operating gasification temperatures, which also result in higher carbon conversion. The hot product gas from the gasifier is cooled upon leaving the gasifier by indirect cooling in gas coolers with external high-pressure steam generation. This mode of cooling operation is selected for applications that require carbon monoxide utilisation later on in the process; e.g., as part of the synthesis gas. (Reimert et al. 2003)

Before utilizing the raw syngas, it needs to be freed of impurities and conditioned. Purification, as an integral part of the syngas production, is required in order to remove impurities such as tar, but also sulphur-containing compounds that are catalyst poisons for WGS catalysts, Fe- or Co-based FT catalysts and also Cu- and Al₂O₃ based MtG and DtG catalysts (Klerk and Furimsky 2010; Baerns 2013). The conditioning process includes the crucial step of adjusting the H₂:CO ratio, which is an important factor for the syngas conversion later on in a synthesis plant. The composition of the synthesis gas can be adjusted in a Water-Gas-Shift (WGS) reactor according to the following reaction.



After the syngas has been conditioned it can be processed through different synthetic processes, but for the concept of synthetic fuel integration into the refinery structures, the Fischer Tropsch, the Methanol-to-Gasoline or the DME-to-Gasoline processes are to be considered. The block diagram in Figure 3 shows the gasification process for syngas production from biomass and the integration of the FT process into the refinery. An air separation unit

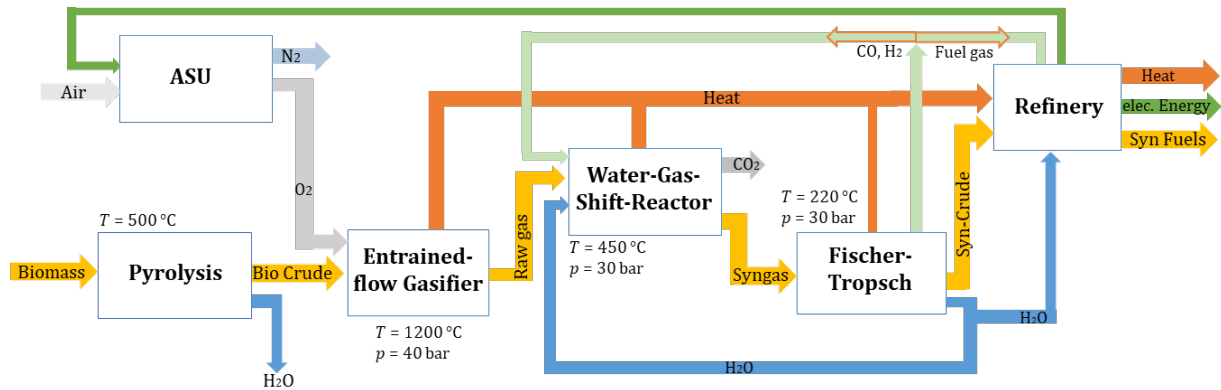


Figure 3. Block diagram of the integration of the gasification system and the FT process in the refinery.

(ASU) provides the gasifier with the required O_2 . Similar block diagrams showing the gasification process and the integration of the MtG and DtG processes in the refinery can be found in the appendix 2.

FISCHER-TROPSCH PROCESS

The Fischer-Tropsch (FT) process, developed in the 1920s, is a classical route for the direct synthesis of liquid hydrocarbons through the direct hydrogenation of CO from the synthesis gas. It constitutes of an exothermic polymerization reaction catalysed with Co or Fe, which results in a linear hydrocarbon product distribution and also water. (Iglesias Gonzalez et al. 2011) The hydrocarbon fraction is commonly referred as a synthetic crude oil, or syncrude, which has to be refined in order to produce useful products, such as transportation fuels and chemicals. The general hydrocarbon distribution produced from the FT reaction is determined through the Anderson-Schulz-Flory (ASF) distribution model. This product distribution can be described by the chain growth probability α , which is the ratio of the of the chain propagation rate r_p and chain termination rate r_t according to the equation:

$$\alpha = \frac{r_p}{r_p + r_t}$$

The choice of the chain growth probability α , which is strongly dependent on the reaction conditions (T, p) and catalyst type, results in the production of hydrocarbons of different boiling ranges as displayed in the following diagram. In this study the value of 0,9 was chosen for the chain growth probability α , because the diesel fraction (C_{10-20}), which is the product fraction with the highest quality in the FT process, has a maximum value when α is around 0,9.

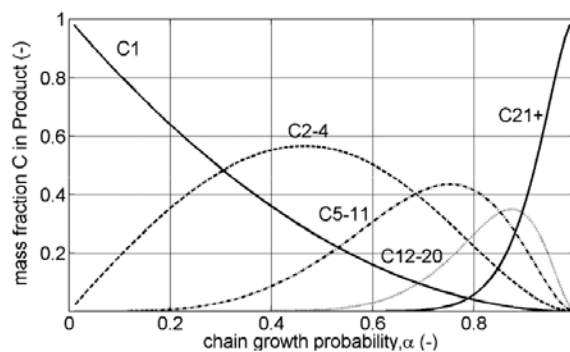


Figure 4. Mass carbon fraction of the different hydrocarbon classes as a function of α , calculated with the ASF model (Iglesias Gonzalez et al. 2011).

The syncrude constitutes the feed to the refinery and as presented in the flowsheet in Figure 5, it is fed into the atmospheric distillation unit and separated into light gases, the gasoline fraction, the diesel fraction and wax. All of these are upgraded to intermediate and final products. The advantage of the diesel fraction of the FT syncrude is its high quality without requirements of upgrading processes, as it can be seen in Figure 5. On the other hand, the gasoline fraction, i.e., raw naphtha needs to be further processed and upgraded in the catalytic reformer (in the presence of H_2) in order to fulfil the required specifications. The lights gases from the syncrude can be processed in the refinery to obtain propylene and refinery gas. Whereas, the wax fraction of the syncrude (C_{20+}) can be converted into lighter boiling fractions through catalytic cracking in the FCC or alternatively through a hydrocracker in the presence of H_2 .

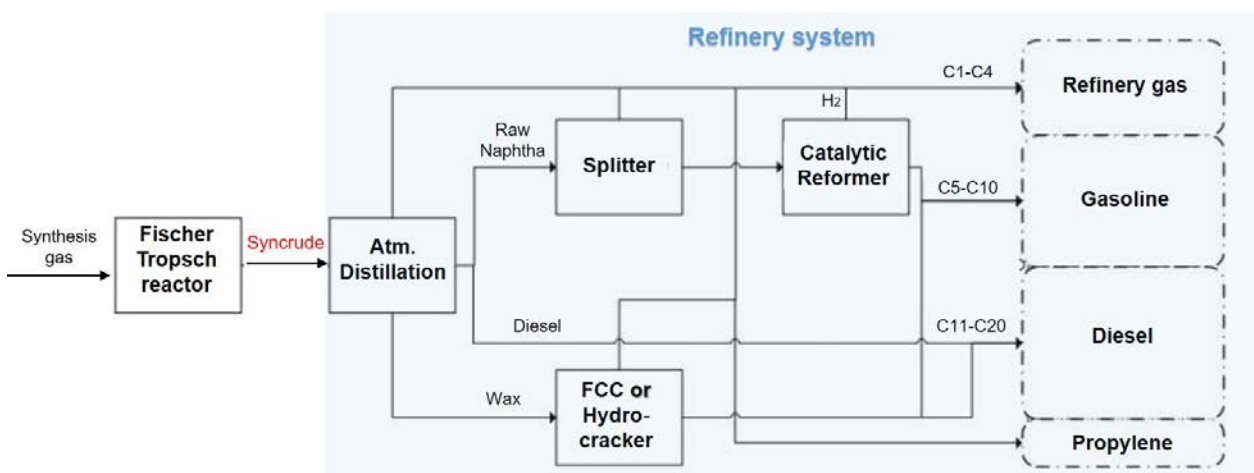


Figure 5. Processing of the FT Syncrude in the refinery structures.

It is important that a clear distinction is made between catalytic cracking and hydrocracking. The latter implies that H_2 is a co-feed, whereas the catalytic cracking in FCC conditions is conducted in the absence of a hydrogen co-feed over monofunctional acidic catalysts. In the hydrocracking process, the basic cracking mechanisms as in the FCC apply, but the catalyst used is bifunctional and the metal sites introduce additional catalytic pathways such as the dehydrogenation of the alkanes in the feed into alkenes, which are then in turn hydrogenated on the acidic sites of the bifunctional catalyst. (Klerk and Furimsky 2010)

METHANOL-TO-GASOLINE AND DME-TO-GASOLINE PROCESSES

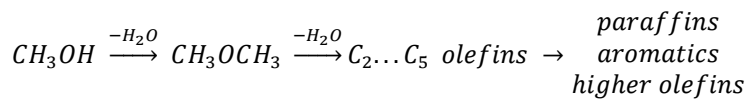
The Methanol-to-Gasoline (MtG) and DME-to-gasoline (DtG) processes are directly linked to the discovery in the 1970s that methanol could be converted into higher hydrocarbons of the gasoline-boiling range over the zeolite ZSM-5 developed in the laboratories of Mobil Oil. ZSM-5 is a medium-pore zeolite, i.e., a crystalline aluminosilicate, with considerable acidity that due to the defined structure and geometry of the pores, channels and cavities is shape-selective and able to control product selectivity so that heavier hydrocarbons, containing more than 11 carbons, are practically not produced. (Bertau et al. 2014) The MtG and DtG processes are indirect catalytic pathways for synthetic fuel production, because the synthesis gas derived from the gasification process is first converted into the intermediate methanol or DME, respectively.

The formation of methanol from synthesis gas on an industrial scale occurs over the catalyst Cu-ZnO-Al₂O₃ at the pressures of 50 - 100 bar and temperatures of 200 - 300 °C (Ott et al. 2003). For a high methanol production, the composition of the synthesis gas is crucial, which can be described through the so-called stoichiometric number:

$$SN = \frac{\dot{N}_{H_2} - \dot{N}_{CO_2}}{\dot{N}_{CO} + \dot{N}_{CO_2}} \approx 2,0 - 2,2$$

DME can be obtained from the catalytic dehydration of MeOH over γ -Al₂O₃. However, for a direct formation of DME from synthesis gas, the utilisation of a bifunctional catalyst is possible, which contains the copper-based catalyst (Cu/ZnO/Al₂O₃), used in the methanol synthesis from syngas, and γ -Al₂O₃, used in the dehydration reaction of methanol into DME. This provides a direct and more economical DME synthesis route (Stiefel et al. 2011), whose feasibility is ascertained even on an industrial scale by companies like JFE Holdings Inc. and Haldor Topsøe A/S (Haro et al. 2013). It has been shown that a H₂:CO ratio in the synthetic gas of 1:1 provides the highest conversion of syngas to DME (Rostrup-Nielsen et al. 2007).

Generally, it is assumed that the reaction of methanol into hydrocarbons of the gasoline boiling range goes according to the following equation, where methanol is firstly dehydrated over ZSM-5 to an equilibrium mixture of DME, methanol and water. Afterwards DME is converted to light olefins, primarily ethylene and propylene, which then undergo further transformation through methylations, oligomerisation and cracking reactions to higher olefins, which in turn produce C₃-C₆ paraffins and C₆-C₁₀ aromatics as end products of cyclization and hydrogen transfer reactions (Chang and Silvestri 1977; Bertau et al. 2014; Olsbye et al. 2012).



The hydrocarbon product selectivity and the catalyst activity are strongly dependent on the

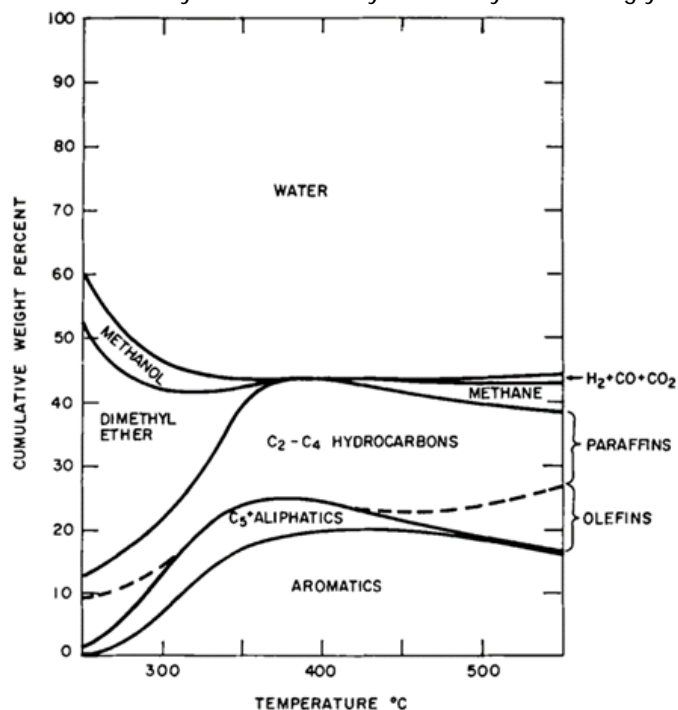


Figure 6. Effect of temperature on the conversion of methanol over ZSM-5 from Chang and Silvestri (1977).

process parameters (T , p and contact time), whereupon these effects are known only from experimental work and data (Bertau et al. 2014). The MtG and DtG processes operate optimally at temperatures between 300 - 450 °C, because at lower temperatures DME does not fully convert, whereas high temperatures lead to higher levels of cracked products such as methane and light olefins, as shown in the Figure 6.

The DME-to-Gasoline (DtG) process is based on the MtG process, since DME, as shown in the reaction above, is an actual intermediate species in the conversion of methanol into hydrocarbons over the ZSM-5 zeolite (Lee et al. 1995). The difference between the MtG and DtG processes consists in the direct synthesis of DME from the syngas upon a bifunctional catalyst and the direct conversion of DME into hydrocarbons of the gasoline-boiling range, without the formation of methanol as an intermediate, as it is the case in the MtG process. It is also important to mention that DME produces an identical hydrocarbon distribution over the ZSM-5 catalyst compared to MeOH (Chang and Silvestri 1977), but the yield produced, i.e. the weight ratio of produced hydrocarbon to water, which is 61 % to 39 %, is higher than in the MtG process of 44 % to 56 % (Gogate 2018; Lee et al. 1995; Fujimoto et al. 1986). In addition, in the DtG process the DME and gasoline reactors are both operated at the same pressure level, whereas in the MtG process two different pressure levels are present. In other words, the DtG process can be considered as a modified version of the MtG process, where the synthesis gas is converted into gasoline in a two-step process, whereas in the MtG process starting from synthesis gas, a three-step process is required. This is illustrated in Figure 7, where the two routes are schematically compared.

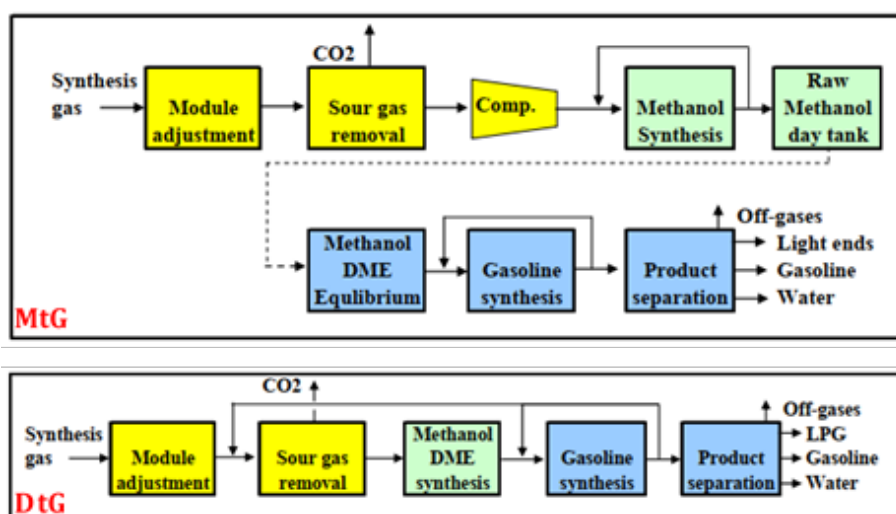


Figure 7. Comparative illustration of the Methanol-to-Gasoline (MtG) and the DME-to-Gasoline (DtG) processes and the raw syngas processing (Rostrup-Nielsen et al. 2007).

The aromatic-rich hydrocarbon mixture derived from the MtG and DtG processes was shown to have a comparable composition to the reformat from the catalytic reformation unit (based on the example of MiRO). For this reason, a processing of the synthetic gasoline blends derived from the MtG and DtG processes in the stabilization column after the reformation unit was undertaken, after some conditioning steps (removal of water from the raw MtG/DtG gasoline, which could lead to corrosion problems in the column). Similar to the processing of the product stream from the reformation unit at MiRO, the stabilization of the synthetic MtG and DtG gasoline blends produces refinery gas, propylene, butane, propane and reformat as displayed in the flowsheet in Figure 8.

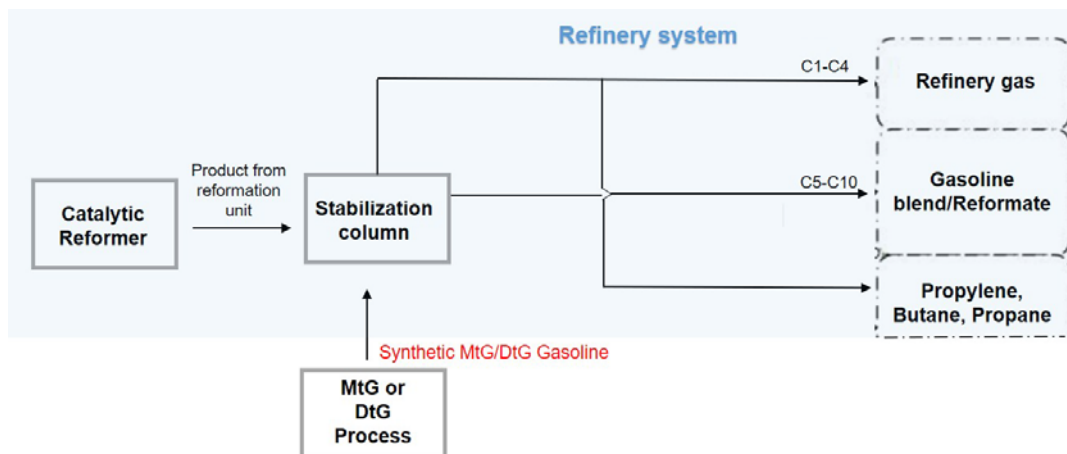


Figure 8. Processing of the MtG and DtG gasoline blends in the refinery structures.

Material and Energy balances

In the calculation of the mass and energy balances in this study, the yield target of syncrude/raw gasoline blend was set at 50 t/h and the following methods/assumptions were applied:

- The pyrolysis, gasification and the WGS-reactors were evaluated based on stoichiometric reactions and efficiency rates based on KIT expertise. The production of synthesis gas was adapted in amount and quality so that the requirements and the target yield for each process pathway (FT, MtG or DtG) could be achieved. As feedstock for the gasification system, wood (chemical formula: $C_6H_9O_4$) was used.
- The Fischer-Tropsch reaction was evaluated based on the Anderson-Schulz-Flory (ASF) distribution model with a chain growth probability α of 0,9. The produced hydrocarbon mixture/syncrude was assumed to be composed only of paraffins. The processing of the syncrude in the refinery structures, as shown in Figure 5, was simulated through an internal simulation software from the KBC company, available at MiRO. The calculations performed in the hydrocracking process display the only exception to this, because they were based on the experimental data from Leckel (2005) derived from the FT process of SASOL (2020). Table A.0.1 in the appendix summarizes the used data. The hydrogen demand of the hydrocracking process was based on the assumption of 20 kg H_2 required per tonne processed wax.
- The Methanol-to-Gasoline and the DME-to-Gasoline processes were simulated through the simulation software ASPEN Plus V10. The conversion of methanol into raw gasoline in the gasoline reactor was evaluated based on the experimental data from Chang and Silvestri (1977), performed on a laboratory scale. In the DtG process simulation these same experimental data were used after being adapted according to the observations of Lee et al. (1995).

Table 1 summarizes the reaction conditions and the assumptions used in the Fischer-Tropsch, the Methanol-to-Gasoline and DME-to-Gasoline processes investigated in this study.

Table 1: Reaction conditions and assumptions used in the Fischer-Tropsch, the Methanol-to-Gasoline and DME-to-Gasoline processes in this study.

Parameter	Fischer Tropsch (FT) process (FT reactor)	Methanol-to-Gasoline (MtG) process (Methanol & Gasoline reactors)		DME-to-Gasoline (DtG) process (DME & Gasoline reactors)	
	Temperature	220 °C	240 °C	350 °C	260 °C
Pressure	30 bar	50 bar	7-10 bar	35 bar	35 bar
Catalyst	Cobalt	Cu-ZnO-Al ₂ O ₃	ZSM-5	γ-Al ₂ O ₃ and Cu-ZnO-Al ₂ O ₃	ZSM-5
H ₂ :CO Ratio	2,1:1	2,2:1	-	1:1	-
Assumptions for hydrocarbon product distribution (at reactor exit)	chain growth probability $\alpha = 0,9$	Hydrocarbon: H ₂ O wt. ratio = 44:56 (Chang and Silvestri 1977)		Hydrocarbon: H ₂ O wt. ratio = 61:39 (Lee et al. 1995)	

FISCHER-TROPSCH PROCESS

In this section the results of the mass and energy balances from the integration of the FT process in the refinery are presented. As displayed in Figure 5, the processing of the waxes of the FT-Syncrude in this study has been analysed based on two different pathways: the catalytic cracking (FCC) and the hydrocracking (HG).

In order to increase the overall efficiency of the processes, in all the production pathways (FT, MtG & DtG) the high temperature sources from the gasification system and the reactors were used for the generation of steam, which was delivered to the refinery. The detailed mass and energy balances in the case of the FT process are presented in the appendix, in Table A.0.5 and Table A.0.6.

For the energy efficiency evaluation of all the processes the following three efficiency factors were used: the synthetic fuel efficiency (η), the product energy efficiency ($\eta_{products}$) and the total energy efficiency (η_{total}). η is defined as the amount of energy, which is stored in the synthetic fuel, i.e., the synthetic diesel and gasoline, in relation to the energy input from the biomass. On the other hand, the product energy efficiency ($\eta_{products}$) includes also the valuable products butane, propane and propylene in the energy efficiency. The overall efficiency of the processes can be estimated based on η_{total} , which considers also other energy sources, such as

by-products, produced steam, refinery gas and electricity, useful for the refinery. The mathematical definitions of these efficiency factors used for the FT process integration are given in the following equations. The results of the mass and energy balances along with the energy efficiencies of the FT process integration (both pathways) are summarized in Table 2.

$$\eta = \frac{(\dot{M} \cdot LHV)_{\text{synthetic gasoline}} + (\dot{M} \cdot LHV)_{\text{synthetic diesel}}}{(\dot{M} \cdot LHV)_{\text{biomass}}}$$

$$\eta_{\text{products}} = \frac{(\dot{M} \cdot LHV)_{\text{synthetic gasoline}} + (\dot{M} \cdot LHV)_{\text{synthetic diesel}} + (\dot{M} \cdot LHV)_{\text{propylene}}}{(\dot{M} \cdot LHV)_{\text{biomass}}}$$

$$\eta_{\text{total}} = \frac{(\dot{M} \cdot LHV)_{\text{synthetic gasoline \& diesel + propylene}} + \dot{Q}_{\text{Steam/District heat/Refinery gas}} + P_{\text{el.}}}{(\dot{M} \cdot LHV)_{\text{biomass}}}$$

Table 2. Mass and energy flows derived from the integration of the FT process (wax processed via FCC or Hydrocracker) and their resulting energy efficiencies.

Mass flow [t/h]	FT (FCC)	FT (HG)	Energy flow [MW]	FT (FCC)	FT (HG)
Input			Input		
Biomass	279,7	286,5	Biomass*	1078,0	1104,0
Biomass (dry)	207,2	212,2			
O ₂ (from air)	96,0	98,4			
Output			Output		
Propylene	0,9	0,0	Steam (3,5/13,5 bar)	346,0	323,0
Synthetic Diesel	19,7	27,5	District heat	0,0	0,0
Synthetic Gasoline	16,8	14,2	Electricity	40,7	33,1
			Propylene & Refinery gas*	12,0	7,5
			Synthetic Diesel*	242,0	337,0
			Synthetic Gasoline*	205,0	174,0
			η [%]	41,5	46,3
			η_{products} [%]	42,6	46,9
* based on the LHV			η_{total} [%]	78,5	79,2

METHANOL-TO-GASOLINE AND DME-TO-GASOLINE PROCESSES

In this section the mass and energy balances from the integration of the MtG and DtG processes in the refinery are shown. The Table A.0.7 and Table A.0.8 in the appendix, present the balances in detail, whereas the Table 3 below summarizes the results and the energy efficiencies. The energy efficiency evaluation of these two processes was performed similar to the FT process integration and is based on the three efficiency factors: synthetic fuel efficiency (η), product energy efficiency ($\eta_{products}$) and total energy efficiency (η_{total}).

$$\eta = \frac{(\dot{M} \cdot LHV)_{stabilized\ gasoline}}{(\dot{M} \cdot LHV)_{biomass}}$$

$$\eta_{products} = \frac{(\dot{M} \cdot LHV)_{stabilized\ gasoline} + (\dot{M} \cdot LHV)_{Butane,propane\ \&\ propylene}}{(\dot{M} \cdot LHV)_{biomass}}$$

$$\eta_{total} = \frac{(\dot{M} \cdot LHV)_{stabilized\ gasoline+LPG} + \dot{Q}_{Steam/District\ heat/Refinery\ gas}}{(\dot{M} \cdot LHV)_{biomass}}$$

Table 3. Mass and energy flows derived from the integration of the MtG and DtG processes and their resulting energy efficiencies.

Mass flow [t/h]	MtG	DtG	Energy flow [MW]	MtG	DtG
Input			Input		
Biomass	351,5	336,1	Biomass*	1354,4	1295,1
Biomass (dry)	260	249,0			
O ₂ (from air)	120,7	115,4			
Output			Output		
Propane	4,4	1,6	Steam (3,5/13,5 bar)	358,7	255,9
Propylene	0,3	0,1	District heat	13,0	28,8
Butane	10,5	5,2	Electricity	3,8	1,2
Synthetic Gasoline blend/Reformate	33,1	37,8	Butane, Propane & Propylene*	193,3	87,3
			Refinery gas*	216,0	47,7
			Synthetic Gasoline blend/Reformate*	392,0	446,1
			η [%]	28,9	34,4
			$\eta_{products}$ [%]	43,2	41,2
* based on the LHV			η_{total} [%]	86,7	66,9

Economic analysis of the integration into the refinery

Lastly a cost analysis of the synthetic fuels produced through the Biomass-to-Liquid route from the Fischer-Tropsch, Methanol-to-Gasoline (MtG) and DME-to-Gasoline (DtG) processes will be shortly presented, all in a scale of 50t/h raw material after the synthesis. The calculated production costs in €/l are based on the synthetic gasoline and diesel for the FT-process and on the synthetic reformat/gasoline blend for the MtG and DtG processes.

The production costs of the synthetic fuels were derived from the summation of the capital expenditures (CAPEX) and the operational expenditures (OPEX). In the evaluation of the CAPEX, the factorial estimation method from Peters et al. (2004) for scaling the costs by capacity was used, because it is difficult to find a published cost estimate for the exact size of the equipment used in this study. In the evaluation of the individual equipment costs, reference equipment data reported from the study of Hannula (2015) were applied. Further details regarding the estimation of the CAPEX can be found in the appendix and the sum of CAPEX data are given in Table 4.

In order to evaluate the OPEX of the production of the synthetic fuels, the utilized raw materials and the maintenance & operating costs need to be considered. The prices of the raw components, by-products and other boundary conditions were based on internal data/experience values from MiRO and KIT.

The following table summarizes the results of the economic analysis for the integration of gasification into the refinery system via the three synthetic fuel production pathways: FT, MtG and DtG.

Table 4. Production costs of the synthetic fuels from the integration of the FT, MtG and DtG processes in the refinery using the Biomass-to-Liquid (BtL) route.

Process route	Fischer-Tropsch	Methanol-to-Gasoline	DME-to-Gasoline
Investment [Mio. €]	1412,4	1381,1	1512,0
Capital expenditures (CAPEX) [€/l]	0,20	0,23	0,22
Operational expenditures (OPEX) [€/l]	0,50	0,52	0,63
BtL- Production costs [€/l]	0,70	0,75	0,85

In addition, as a comparison also the production costs for the integration of the Power-to-Liquid (PtL) route were considered and are presented in the Table 5. These costs were estimated first, for an ideal production site in Germany and second, using the assumption that the renewable electricity was produced in the favourable Middle East and North Africa (MENA) regions. The latter had lower process OPEX compared to a PtL process operated, e.g., at Germany. The comparison between the production costs of the two routes shows that the Power-to-Liquid route would be competitive to the Biomass-to-Liquid route only under favourable electricity production conditions. Costs for Electricity in Germany were estimated with 40€/MWh and in MENA region with 15€/MWh.

Table 5. Production costs of the synthetic fuels from the integration of the FT, MtG and DtG processes in the refinery using the Power-to-Liquid (PtL) route.

Process route	Fischer-Tropsch	Methanol-to-Gasoline	DME-to-Gasoline
CAPEX PtL [€/l]	0,31	0,40	0,43
OPEX PtL Germany [€/l]	1,02	1,08	1,28
PtL Germany - Production costs [€/l]	1,33	1,48	1,71
OPEX PtL MENA regions [€/l]	0,40	0,23	0,37
PtL MENA regions - Production costs [€/l]	0,71	0,63	0,80

Appendices

Appendix 1 - Tables

Table A.0.1. Experimental data for the hydrocarbon distribution of the hydrocracked FT-wax product from (Leckel 2005).

Table 5. Hydrocracking of Hydrogenated (H) and Unhydrogenated Iron-Catalyzed FT Slurry Bed Reactor Wax at 7.0 MPa, 0.55h⁻¹ LHSV, and a H₂/Wax Ratio of 1500/1 L_n/L

T, °C	C ₂₃₊ conv., wt %	selectivity, wt %			yield, wt %		
		C ₁ -C ₄	C ₅ -C ₉	C ₁₀ -C ₂₂	C ₁ -C ₄	C ₅ -C ₉	C ₁₀ -C ₂₂
360 (H)	70	2.7	30	68	1.9	21	48
365 (H)	83	3.4	30	66	2.8	25	55
370 (H)	99	3.9	38	59	3.9	38	58
375 (H)	100	4.8	41	54	4.8	41	54
360	25	3.7	19	76	0.9	4.7	19
375	69	4.1	20	74	2.8	14	51
380	97	7.6	34	58	7.4	33	56

Table A.0.2. Zeolite-Catalysed Hydrocarbon Formation from Methanol based on Chang and Silvestri (1977).

Reactant:	Methanol	<i>t</i> -Butanol	1-Heptanol	Methanethiol	Propanal	Methylal
Reaction conditions						
T (°C)	371	371	371	482	371	371
LHSV (hr ⁻¹)	1.0	1.0	0.7	1.0	1.0	1.0
Conversion (%)	100.0	100.0	99.9	99.9 ^a	99.9	100.0 ^b
Hydrocarbon distribution (wt%)						
Methane	1.0	0.1	0.0	6.6	0.8	1.5
Ethane	0.6	0.7	0.3	8.3	0.4	0.7
Ethylene	0.5	0.5	<0.1	6.7	0.4	0.3
Propane	16.2	18.8	16.4	15.3	7.3	16.4
Propylene	1.0	1.1	0.2	1.3	0.6	0.9
<i>i</i> -Butane	18.7	18.4	19.3	9.0	4.6	15.1
<i>n</i> -Butane	5.6	8.6	11.0	3.1	3.0	5.8
Butenes	1.3	0.7	<0.1	0.2	0.3	0.9
<i>i</i> -Pentane	7.8	6.2	8.7	1.2	1.8	5.8
<i>n</i> -Pentane	1.3	1.4	1.5	<0.1	0.6	1.0
Pentenes	0.5	0.2	0.1	<0.1	0.2	0.2
C ₆ ⁺ aliphatics	4.3	7.6	3.0	0.1	1.3	3.2
Benzene	1.7	3.3	3.4	0.2	4.1	1.1
Toluene	10.5	11.6	14.3	1.3	23.7	7.9
Ethylbenzene	0.8	1.3	1.2	<0.1	2.6	0.7
Xylenes	17.2	12.4	11.6	8.9	26.4	20.5
C ₉ Aromatics	7.5	6.1	5.3	27.0	18.6	12.4
C ₁₀ Aromatics	3.3	0.4	2.9	9.5	3.7	5.4
C ₁₁ ⁺ Aromatics	0.2	0.6	0.6	1.3	0.6	0.2

Table A.0.3. Aromatics Distribution from the Methanol conversion displayed in Table A.0.2.

	Normalized distribution (wt%)	Normalized isomer distributions	Equilibrium distributions (371°C)
Benzene	4.1		
Toluene	25.6		
Ethylbenzene	1.9		
Xylenes			
<i>o</i>	9.0	[21.5]	[23.8]
<i>m</i>	22.8	[54.6]	[52.7]
<i>p</i>	10.0	[23.9]	[23.5]
Trimethylbenzenes			
1,2,3	0.9	[6.4]	[7.8]
1,2,4	11.1	[78.7]	[66.0]
1,3,5	2.1	[14.9]	[26.2]
Ethyltoluenes			
<i>o</i>	0.7		
<i>m + p</i>	4.1		
Isopropylbenzene	0.2		
Tetramethylbenzenes			
1,2,3,4	0.4	[23.3]	[16.0]
1,2,3,5	1.9	[44.2]	[50.6]
1,2,4,5	2.0	[46.5]	[33.4]
Other A ₁₀ ^b	2.7		
A ₁₁ ⁺	0.4		

^a See Table 1, Example 1.

^b Diethylbenzenes + dimethylethylbenzenes.

Table A.0.4. Effect of Space Velocity on Methanol Conversion and Hydrocarbon Distribution from Chang and Silvestri (1977).

LHSV	1080	108	1
[vol of liquid methanol/ (vol of catalyst/hr)]			
Product distribution (wt%)			
Water	8.9	33.0	56.0
Methanol	67.4	21.4	0.0
Dimethyl ether	23.5	31.0	0.0
Hydrocarbons	0.2	14.6	44.0
Conversion (MeOH + MeOMe) (wt%)	9.1	47.5	100.0
Hydrocarbon distribution (wt%)			
Methane	1.5	1.1	1.1
Ethane	—	0.1	0.6
Ethylene	18.1	12.4	0.5
Propane	2.0	2.5	16.2
Propylene	48.2	26.7	1.0
<i>i</i> -Butane	13.8	6.5	18.7
<i>n</i> -Butane	—	1.3	5.6
Butenes	11.9	15.8	1.3
C ₅ ⁺ Aliphatics	4.4	27.0	14.0
Aromatics	—	6.6	41.1

Table A.0.5. Mass and energy balance of the FT process integration (Wax processed in the FCC).

Mass balance

Unit	C ₆ H ₉ O ₄ (wet)	C ₆ H ₉ O ₄ (dry)	Pyrolysis slurry	H ₂	H ₂ O	Air	N ₂	O ₂	CO ₂	CO	Wax	Refinery gas	Diesel	Gasoline	Propylene
Drying	-279,7 t/h	207,2 t/h			72,5 t/h										
Fast Pyrolysis	-207,2 t/h		118,6 t/h												
Gasifier			-118,6 t/h	8,9 t/h	-10,3 t/h			-96,0 t/h	44,0 t/h	172,1 t/h					
WGS				5,2 t/h	-47,1 t/h				115,1 t/h	-73,3 t/h					
ASU						-457,3 t/h	361,3 t/h	96,0 t/h							
FT				-14,8 t/h	63,3 t/h					-98,5 t/h		50 t/h Syncrude			
Distillation											17,1 t/h	4,7 t/h	17,4 t/h	10,8 t/h	
Reformer				0,7 t/h								2,5 t/h		7,6 t/h	
FCC											-17,1 t/h	4,7 t/h	2,3 t/h	9,2 t/h	0,9 t/h
Total to refinery	-279,7 t/h		0,0t/h	0,0t/h	78,4 t/h	-457,3 t/h	361,3 t/h	0,0t/h	159,2 t/h	0,2 t/h	0,0 t/h	11,9 t/h	19,7 t/h	16,8 t/h	0,9 t/h

Energy balance

Unit	Electricity			Heat			C ₆ H ₉ O ₄ (dry)	Pyrolysis slurry	H ₂	CO	Wax	Refinery gas	Diesel	Gasoline	Propylene
	Own consumption	Loss	Prod.	Own consumption	Process	Production									
Fast Pyrolysis				-5 MW	-108 MW*		-1078 MW	965 MW							
Gasifier					184 MW			-965 MW	298 MW	483 MW					
WGS					30 MW				202 MW	-191 MW					
ASU	-29 MW														
Steam Power plant			70 MW	-25 MW	-367 MW	410 MW						-138 MW			
FT					153 MW				-522 MW	-291 MW		56 MW			
Distillation				-34 MW							210 MW	61 MW	215 MW	135 MW	
Reformer									23 MW			17 MW		93 MW	
FCC											-210 MW	60 MW	27 MW	112 MW	12 MW
Total to refinery		41 MW			346 MW		-1078 MW	0 MW	0 MW	1 MW		0 MW	242 MW	205 MW	12 MW

* The heat required for drying the biomass up and achieving the high temperature in the fast pyrolysis reactor is internally generated by burning the pyrolysis gas.

Table A.0.6. Mass and energy balance of the FT process integration (Wax processed in the Hydrocracker).

Mass balance

Unit	C ₆ H ₉ O ₄ (wet)	C ₆ H ₉ O ₄ (dry)	Pyrolysis slurry	H ₂	H ₂ O	Air	N ₂	O ₂	CO ₂	CO	Wax	Refinery gas	Diesel	Gasoline
Drying	-286,5 t/h	212,2 t/h			74,3 t/h									
Fast Pyrolysis	-212,2 t/h		121,5 t/h											
Gasifier			-121,5 t/h	9,1 t/h	-10,5 t/h			-98,4 t/h	45,1 t/h	176,2 t/h				
WGS				5,4 t/h	-48,2 t/h				117,9 t/h	-75,1 t/h				
ASU						-468,4 t/h	370,0 t/h	98,4 t/h						
FT				-14,8 t/h	63,3 t/h					-98,5 t/h		50 t/h Syncrude		
Distillation											17,1 t/h	4,7 t/h	17,4 t/h	10,8 t/h
Reformer				0,7 t/h								2,5 t/h		7,6 t/h
Hydrocracker				-3,0 t/h							-17,1 t/h	0,7 t/h	10,1 t/h	6,6 t/h
Total to refinery	-286,5 t/h		0,0t/h	0,0t/h	78,8 t/h	-468,4 t/h	370,0 t/h	0,0t/h	163,0 t/h	2,7 t/h	0,0 t/h	8,0 t/h	27,5 t/h	14,2 t/h

Energy balance

Unit	Electricity			Heat			C ₆ H ₉ O ₄ (dry)	Pyrolysis slurry	H ₂	CO	Wax	Refinery gas	Diesel	Gasoline
	Own consumption	Loss	Prod.	Own consumption	Process	Production								
Fast Pyrolysis				-5 MW	-111 MW*		-1104 MW	988 MW						
Gasifier					188 MW			-988 MW	305 MW	495 MW				
WGS					31 MW				206 MW	-196 MW				
ASU	-30 MW													
Steam Power plant			63 MW	-23 MW	-372 MW	422 MW						-87 MW		
FT					153 MW				-522 MW	-291 MW		56 MW		
Distillation				-34 MW							210 MW	61 MW	215 MW	135 MW
Reformer									23 MW			17 MW		93 MW
Hydrocracker						9 MW			-11 MW		-210 MW	9 MW	122 MW	81 MW
Total to refinery		33 MW			323 MW		-1104 MW	0 MW	0 MW	8 MW		0 MW	337 MW	174 MW

* The heat required for drying the biomass up and achieving the high temperature in the fast pyrolysis reactor is internally generated by burning the pyrolysis gas.

Table A.0.7. Mass and energy balance of the MtG process integration in the refinery.

Mass balance

Unit	C ₆ H ₉ O ₄ (wet)	C ₆ H ₉ O ₄ (dry)	Pyrolysis slurry	H ₂	H ₂ O	Air	N ₂	O ₂	CO ₂	CO	Butane	Propane	Gasoline blend/Reformate	Propylene
Drying	-351,5 t/h	260,4 t/h			91,1 t/h									
Fast Pyrolysis	-260,4 t/h		149,0 t/h		50,1 t/h									
Gasifier			-149,0 t/h	11,1 t/h	-12,9 t/h			-120,7 t/h	55,3 t/h	216,2 t/h				
WGS				6,6 t/h	-59,2 t/h				144,6 t/h	-92,0 t/h				
ASU						-574,6 t/h	454,0 t/h	120,7 t/h						
MtG Process				-17,7 t/h	111,2 t/h				-26,5 t/h	-120,4 t/h	50 t/h Raw MtG-Gasoline blend			
Stabilization column											10,5 t/h	4,4 t/h	33,1 t/h	0,3 t/h
Total to refinery	-351,5 t/h		0,0 t/h	0,0 t/h	180,3 t/h	-574,6 t/h	454,0 t/h	0,0 t/h	173,4 t/h	3,8 t/h	10,5 t/h	4,4 t/h	33,1 t/h	0,3 t/h

Energy balance

Unit	Electricity			Heat								C ₃₋₄		
	Own consumption	Loss	Prod.	Own consumption	Process	Production	District heat	C ₆ H ₉ O ₄ (dry)	Pyrolysis slurry	H ₂	CO		Refinery gas	Gasoline blend/Reformate
Fast Pyrolysis				-7 MW	-136 MW*			-1354 MW	1212 MW					
Gasifier					231 MW				-1212 MW	374 MW	607 MW			
WGS					38 MW					220 MW	-259 MW			
ASU	-36 MW													
Steam Power plant			40 MW	-13MW	-269 MW	209 MW								
MtG Process						169,7 MW	13 MW			-594 MW	-338 MW	205,3 MW		
Stabilization column													392,0 MW	193,4 MW
Total to refinery		4 MW			371,7 MW			-1354 MW	0 MW	0 MW	11 MW	205,3 MW	392,0 MW	193,4 MW

* The heat required for drying the biomass up and achieving the high temperature in the fast pyrolysis reactor is internally generated by burning the pyrolysis gas.

Table A.0.8. Mass and energy balance of the DtG process integration in the refinery.

Mass balance

Unit	C ₆ H ₉ O ₄ (wet)	C ₆ H ₉ O ₄ (dry)	Pyrolysis slurry	H ₂	H ₂ O	Air	N ₂	O ₂	CO ₂	CO	Butane	Propane	Gasoline blend/Reformate	Propylene
Drying	-336,1 t/h	249,0 t/h			87,1 t/h									
Fast Pyrolysis	-249,0 t/h		142,5 t/h		47,9 t/h									
Gasifier			-142,5 t/h	10,6 t/h	-12,4 t/h			-115,4 t/h	52,9 t/h	206,7 t/h				
WGS				2,1 t/h	-19,2 t/h									
ASU						-549,5 t/h	434,1 t/h	115,4 t/h	47,0 t/h	-29,9 t/h				
DtG Process				-12,8 t/h	83,6 t/h				-24,2 t/h	-176,9 t/h	50 t/h Raw DtG-Gasoline blend			
Stabilization column											5,2 t/h	1,6 t/h	37,8 t/h	0,1 t/h
Total to refinery	-336,1 t/h		0,0 t/h	0,0 t/h	187,1 t/h	-549,5 t/h	434,1 t/h	0,0 t/h	75,7 t/h	0,0 t/h	5,2 t/h	1,6 t/h	37,8 t/h	0,1 t/h

Energy balance

Unit	Electricity			Heat				C ₆ H ₉ O ₄ (dry)	Pyrolysis slurry	H ₂	CO	Refinery gas	Gasoline blend/Reformate	C ₃₋₄
	Own consumption	Loss	Prod.	Own consumption	Process	Production	District heat							
Fast Pyrolysis				-6 MW	-130 MW*			-1295,1 MW	1159 MW					
Gasifier					221 MW				-1159 MW	359 MW	581 MW			
WGS					12 MW					72 MW	-84 MW			
ASU	-35 MW													
Steam Power plant			36 MW	-12 MW	-233 MW	180 MW								
DtG Process					-92,1 MW	186 MW	28,8 MW			-429 MW	-497 MW	47,7 MW		
Stabilization column													446,1 MW	87,3 MW
Total to refinery		1 MW			284,7 MW			-1295,1 MW	0 MW	0 MW	0 MW	47,7 MW	446,1 MW	87,3 MW

* The heat required for drying the biomass up and achieving the high temperature in the fast pyrolysis reactor is internally generated by burning the pyrolysis gas.

Appendix 2 - Figures & Further details

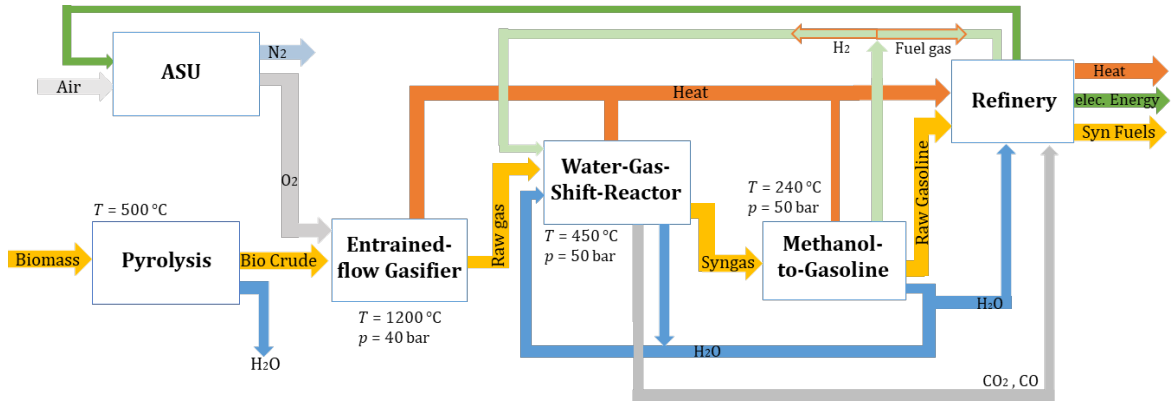


Figure A.0.9. Block diagram of the integration of the gasification system and the MtG process in the refinery.

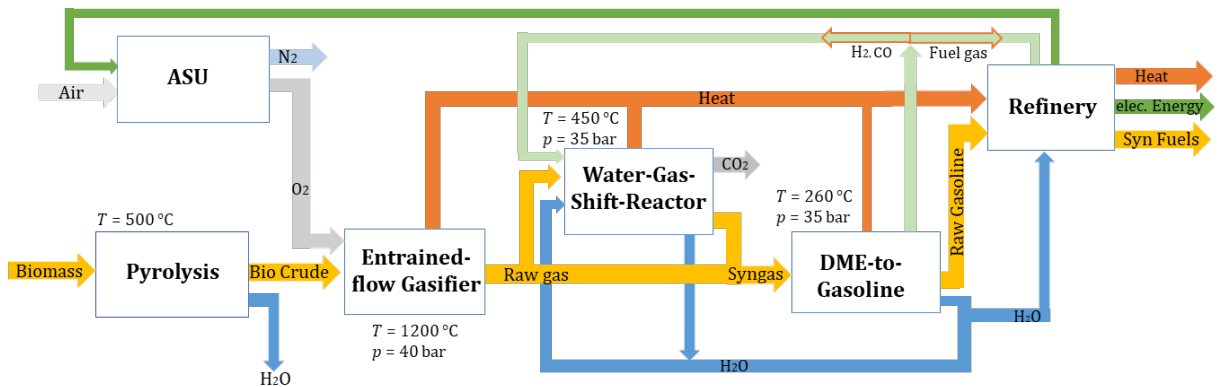


Figure A.0.10. Block diagram of the integration of the gasification system and the DtG process in the refinery.

CAPEX estimation

$$I = \sum_i \left[I_0 * \left(\frac{S}{S_0} \right)^k * (1 + IDC + PC) \right]_i$$

$$CAPEX = I * (1 + f_{equ.} + f_a + f_p + f_{Interest})$$

I_0 describes the cost estimate of a reference equipment, whereas the fraction $\frac{S}{S_0}$ sets the ratio between the capacities of a target plant (here at MiRO) to that of the reference equipment. The cost scaling factor k , also taken from literature data, is used to optimally depict the scale-up of the costs. The IDC and PC factors are added in the equation in order to consider the indirect costs and project risks into the evaluation.

Apart from the total investment cost I , also additional charges need to be considered in the evaluation of the total CAPEX, as shown in the second equation above. The additional charges include the extra costs of equipment, montage and start-up operations, loan interest, administration, personal etc. In the estimation also the depreciation effects were incorporated, with a time of 10 years, 5 % interest rate and an average production time of 8600 h/a.

Table A.0.9. Details of CAPEX for BtL routes

Process route	Fischer-Tropsch	Methanol-to-Gasoline	DME-to-Gasoline
Pyrolysis unit [Mio. €]	56,7	69,6	66,8
Entrained flow gasifier [Mio. €]	338,6	384,9	369,7
WGS unit [Mio. €]	12,5	16,5	6,0
Synthesis unit [Mio. €]	185,8	109,4	192,9
Investment [Mio. €]	593,6	580,4	635,4
+Σ additional charges	818,8	800,7	876,6

Total Investment [Mio. €]	1412,4	1381,1	1512,0
---------------------------	--------	--------	--------

Index of Tables

Table 1: Reaction conditions and assumptions used in the Fischer-Tropsch, the Methanol-to-Gasoline and DME-to-Gasoline processes in this study.	14
Table 2. Mass and energy flows derived from the integration of the FT process (wax processed via FCC or Hydrocracker) and their resulting energy efficiencies.	15
Table 3. Mass and energy flows derived from the integration of the MtG and DtG processes and their resulting energy efficiencies.	17
Table 4. Production costs of the synthetic fuels from the integration of the FT, MtG and DtG processes in the refinery using the Biomass-to-Liquid (BtL) route.	19
Table 5. Production costs of the synthetic fuels from the integration of the FT, MtG and DtG processes in the refinery using the Power-to-Liquid (PtL) route.	20
Table A.0.1. Experimental data for the hydrocarbon distribution of the hydrocracked FT-wax product from (Leckel 2005).	21
Table A.0.2. Zeolite-Catalyzed Hydrocarbon Formation from Methanol based on Chang and Silvestri (1977).	21
Table A.0.3. Aromatics Distribution from the Methanol conversion displayed in Table A.0.2.	22
Table A.0.4. Effect of Space Velocity on Methanol Conversion and Hydrocarbon Distribution from Chang and Silvestri (1977).	22
Table A.0.5. Mass and energy balance of the FT process integration (Wax processed in the FCC).	23
Table A.0.6. Mass and energy balance of the FT process integration (Wax processed in the Hydrocracker).	24
Table A.0.7. Mass and energy balance of the MtG process integration in the refinery.	25
Table A.0.8. Mass and energy balance of the DtG process integration in the refinery.	26

Index of Figures

Figure 1. Block diagram of main refinery structures at MiRO.....	5
Figure 2. Summary of different pathways for the production of synthetic fuels.....	7
Figure 3. Block diagram of the integration of the gasification system and the FT process in the refinery.....	9
Figure 4. Mass carbon fraction of the different hydrocarbon classes as a function of α , calculated with the ASF model (Iglesias Gonzalez et al. 2011).....	9
Figure 5. Processing of the FT Syncrude in the refinery structures.	10
Figure 6. Effect of temperature on the conversion of methanol over ZSM-5 from Chang and Silvestri (1977).	11
Figure 7. Comparative illustration of the Methanol-to-Gasoline (MtG) and the DME-to-Gasoline (DtG) processes and the raw syngas processing (Rostrup-Nielsen et al. 2007).	12
Figure 8. Processing of the MtG and DtG gasoline blends in the refinery structures.	13
Figure A.0.1. Block diagram of the integration of the gasification system and the MtG process in the refinery.....	27
Figure A.0.2. Block diagram of the integration of the gasification system and the DtG process in the refinery.....	27

Publication bibliography

Alfke, Gunter; Irion, Walther W.; Neuwirth, Otto S. (2003): Oil Refining. In : Ullmann's encyclopedia of industrial chemistry. 6th, completely rev. ed. Weinheim, Germany: Wiley-VCH.

DIN EN 590:2017-10, 2017: Automotive fuels - Diesel - Requirements and test methods; German version EN 590:2013+A1:2017.

DIN EN 228:2017-08, 2017: Automotive fuels - Unleaded petrol - Requirements and test methods; German version EN 228:2012+A1:2017.

Baerns, Manfred (2013): Technische Chemie. Zweite, erweiterte Auflage. Weinheim: Wiley-VCH (ebrary online). Available online at <http://search.ebscohost.com/login.aspx?direct=true&scope=site&db=nlebk&db=nlabk&AN=878369>.

Bertau, Martin; Offermanns, Heribert; Plass, Ludolf; Schmidt, Friedrich; Wernicke, Hans-Jürgen; Asinger, Friedrich (2014): Methanol. The basic chemical and energy feedstock of the future : Asinger's vision today ; based on "Methanol - Chemie- und Energierohstoff: die Mobilisation der Kohle" by Friedrich Asinger published in 1986. Berlin: Springer. Available online at <http://gbv.ebib.com/patron/FullRecord.aspx?p=1698208>.

BMW (2010): Energiekonzept für eine umweltschonende, zuverlässige und bezahlbare Energieversorgung. Available online at <https://www.bmw.de/Redaktion/DE/Downloads/E/energiekonzept-2010.html>.

Chang, C.; Silvestri, A. (1977): The conversion of methanol and other O-compounds to hydrocarbons over zeolite catalysts. In *Journal of Catalysis* 47 (2), pp. 249-259. DOI: 10.1016/0021-9517(77)90172-5.

Dabelstein, Werner; Reglitzky, Arno; Schütze, Andrea; Reders, Klaus; Brunner, Andreas (2003): Automotive Fuels. In : Ullmann's encyclopedia of industrial chemistry. 6th, completely rev. ed. Weinheim, Germany: Wiley-VCH, pp. 1-41.

Dahmen, Nicolaus; Abeln, Johannes; Eberhard, Mark; Kolb, Thomas; Leibold, Hans; Sauer, Jörg et al. (2017): The bioliq process for producing synthetic transportation fuels. In *WIREs Energy Environ* 6 (3), e236. DOI: 10.1002/wene.236.

Dietrich, Ralph-Uwe; Albrecht, Friedemann; Pregger, Thomas (2018): Erzeugung alternativer flüssiger Kraftstoffe im zukünftigen Energiesystem. In *Chemie Ingenieur Technik* 90 (1-2), pp. 179-192. DOI: 10.1002/cite.201700090.

Dimitriou, Ioanna; Goldingay, Harry; Bridgwater, Anthony V. (2018): Techno-economic and uncertainty analysis of Biomass to Liquid (BTL) systems for transport fuel production. In *Renewable and Sustainable Energy Reviews* 88, pp. 160-175. DOI: 10.1016/j.rser.2018.02.023.

Fujimoto, Kaoru; Asami, Kenji; Saima, Hitoshi; Shikada, Tsutomu; Tominaga, Hiroo (1986): Two-stage reaction system for synthesis gas conversion to gasoline. In *Ind. Eng. Chem. Prod. Res. Dev.* 25 (2), pp. 262-267. DOI: 10.1021/i300022a023.

Gary, James H.; Kaiser, Mark J.; Klerk, Arno. de; Handwerk, Glenn E. (2020): Petroleum refining. Technology, economics, and markets. Sixth edition. Boca Raton, FL: CRC Press/Taylor & Francis Group.

Gogate, Makarand R. (2018): The direct, one-step process for synthesis of dimethyl ether from syngas. III. DME as a chemical feedstock. In *Petroleum Science and Technology* 36 (8), pp. 562-568. DOI: 10.1080/10916466.2018.1428630.

Hannula, Ilkka (2015): Co-production of synthetic fuels and district heat from biomass residues, carbon dioxide and electricity: Performance and cost analysis. In *Biomass and Bioenergy* 74, pp. 26-46. DOI:

10.1016/j.biombioe.2015.01.006.

Haro, Pedro; Trippe, Frederik; Stahl, Ralph; Henrich, Edmund (2013): Bio-syngas to gasoline and olefins via DME - A comprehensive techno-economic assessment. In *Applied Energy* 108, pp. 54-65. DOI: 10.1016/j.apenergy.2013.03.015.

Hobohm, Jens; Maur, Alex auf der; Dambeck, Hans; Kemmler, Andreas (2018): Status Und Perspektiven Flüssiger Energieträger In Der Energiewende. Eine Studie der Prognos AG, des Fraunhofer-Instituts für Umwelt-, Sicherheits- und Energie-technik. Mineralölwirtschaftsverband e.V. (MWV), Institut für Wärme und Oeltechnik e.V. (IWO), MEW Mittelständische Energiewirtschaft Deutschland e.V., UNITI Bundesverband mittelständischer, Mineralölunternehmen e. V. Available online at https://www.mwv.de/wp-content/uploads/2019/11/191101-Prognos-Endbericht_Fluessige_Energietraeger_Web-2.-Auflage.pdf.

Iglesias Gonzalez, Maria; Kraushaar-Czarnetzki, Bettina; Schaub, Georg (2011): Process comparison of biomass-to-liquid (BtL) routes Fischer-Tropsch synthesis and methanol to gasoline. In *Biomass Conv. Bioref.* 1 (4), pp. 229-243. DOI: 10.1007/s13399-011-0022-2.

Jung, Constanze; Seifert, Peter; Mehlhose, Friedemann; Hahn, Christoph; Schröder, Daniel; Wolfersdorf, Christian et al. (2020): Ottokraftstoffe aus erneuerbarem Methanol. In *Chemie Ingenieur Technik* 92 (1-2), pp. 100-115. DOI: 10.1002/cite.201900108.

Klerk, Arno; Furimsky, Edward (2010): Catalysis in the Refining of Fischer-Tropsch Syncrude. Cambridge: Royal Society of Chemistry.

Leckel, Dieter (2005): Hydrocracking of Iron-Catalyzed Fischer-Tropsch Waxes. In *Energy Fuels* 19 (5), pp. 1795-1803. DOI: 10.1021/ef050085v.

Lee, Sunggyu; Gogate, Makarand; Kulik, Conrad J. (1995): METHANOL-TO-GASOLINE VS. DME-TO-GASOLINE II. PROCESS COMPARISON AND ANALYSIS. In *Fuel Science and Technology International* 13 (8), pp. 1039-1057. DOI: 10.1080/08843759508947721.

Liederman, David; Yurchak, Sergei; Kuo, James C. W.; Lee, Wooyoung (1982): Mobil Methanol-to-Gasoline Process. In *Journal of Energy* 6 (5), pp. 340-341. DOI: 10.2514/3.62614.

MiRO Mineraloelraffinerie Oberrhein (2021): Fließbild Produkte & Prozesse. Available online at <https://www.miro-ka.de/de/produkte-prozesse.htm>.

MWV (2017): Jahresbericht 2017. Mineralölwirtschaftsverband e.V. (MWV). Available online at https://www.mwv.de/wp-content/uploads/2017/09/170918_Mineraloelwirtschaftsverband_Jahresbericht-2017.pdf.

Olah, George A.; Goeppert, Alain; Prakash, G. K. Surya (2006): Beyond Oil and Gas: the methanol economy. Weinheim: Wiley-VCH. Available online at <http://search.ebscohost.com/login.aspx?direct=true&scope=site&db=nlebk&db=nlabk&AN=169587>.

Olsbye, Unni; Svelle, Stian; Bjørgen, Morten; Beato, Pablo; Janssens, Ton V. W.; Joensen, Finn et al. (2012): Conversion of methanol to hydrocarbons: how zeolite cavity and pore size controls product selectivity. In *Angewandte Chemie (International ed. in English)* 51 (24), pp. 5810-5831. DOI: 10.1002/anie.201103657.

Ott, Jörg; Gronemann, Veronika; Pontzen, Florian; Fiedler, Eckhard; Grossmann, Georg; Kersebohm, D. Burkhard et al. (2003): Methanol. In : Ullmann's encyclopedia of industrial chemistry. 6th, completely rev. ed. Weinheim, Germany: Wiley-VCH.

Peters, Max Stone; Timmerhaus, Klaus Dieter; West, Ronald Emmett (2004): Plant design and economics for chemical engineers. Boston: McGraw-Hill.

Reimert, Rainer; Marschner, Friedemann; Renner, Hans-Joachim; Boll, Walter; Supp, Emil; Brejc, Miron et al. (2003): Gas Production, 2. Processes. In : Ullmann's encyclopedia of industrial chemistry. 6th, completely rev. ed. Weinheim, Germany: Wiley-VCH.

Rostrup-Nielsen, T.; Hoejlund Nielsen, P. E.; Joensen, Finn; Madsen, Joergen. (2007): Polygeneration - Integration of gasonline synthesis and IGCC power production using Topsoe's TIGAS process. Forskningscenter Risø; Risø International Energy Conference 2007. Denmark: Roskilde.

SASOL (2020): Overview | Sasol. Available online at <https://www.sasol.com/about-sasol/regional-operating-hubs/southern-africa-operations/secunda-synfuels-operations/overview>, updated on 9/27/2020.000Z, checked on 9/27/2020.809Z.

Stiefel, Miriam; Ahmad, Ruaa; Arnold, Ulrich; Döring, Manfred (2011): Direct synthesis of dimethyl ether from carbon-monoxide-rich synthesis gas: Influence of dehydration catalysts and operating conditions. In *Fuel Processing Technology* 92 (8), pp. 1466-1474. DOI: 10.1016/j.fuproc.2011.03.007.

Tunå, Per; Hulteberg, Christian (2014): Woody biomass-based transportation fuels - A comparative techno-economic study. In *Fuel* 117, pp. 1020-1026. DOI: 10.1016/j.fuel.2013.10.019.



IEA Bioenergy
Technology Collaboration Programme